Automatic alignment system for optical lithography based on machine vision

HUANG Tao [a], LIU Shiyuan [*, a], YI Pengxing [a], SHI Tielin [b]
[a] State Key Laboratory of Digital Manufacturing Equipment and Technology, Huazhong University of Science and Technology, Wuhan, China.
[b] Wuhan National Laboratory for Optoelectronics, Huazhong University of Science and Technology, Wuhan, China.

ABSTRACT

This paper presents an automatic alignment system based on machine vision method. A high-speed gray pattern match algorithms is proposed based on the combination of sequential similarity detection algorithm (SSDA) and multiresolution pagoda structure algorithm (MPSA). A dynamic system calibration model suitable for the algorithm automatic alignment system is established to relate the pixel coordinate in CCD to the physical coordinate, which is based on Tsai's two-step algorithm but with the help of precise positioning of the wafer stage in X-Y directions. A lot of experiments conducted on a machine vision experimental platform confirm that the proposed technique is feasible and effective. The pattern match algorithm is demonstrated to achieve an error less than one-twentieth pixels, while the computation time is shorter than 200ms when using a large pattern image with 320×320 pixels. The absolute alignment error is illustrated to be lower than 200nm within a large field of view of 1mm×1mm after the platform is calibrated using the proposed dynamic calibration method.

Keywords: Lithography, Alignment, pattern match, Image processing, Machine vision.

1. INTRODUCTION

Automatic alignment system is one of the key subsystems in optical lithography tools. Compared with other methods, machine vision based alignment has many advantages, such as high precision, process intuitive, simple structure, and high efficiency [1-6]. Therefore, it has been widely used in many applications including in optical lithography tools. In this case, improving the machine vision accuracy directly results in the improving of the overlay, and the alignment speed and efficiency affect the throughput. The key technologies include target pattern extraction, pattern matching and camera calibration. A number of research institutions and companies have developed their commercial imaging processing products, such as Patmax by Congex and EasyMatch by Euresys, which have applications in semiconductor industry [8, 9]. Patmax is a geometric pattern-matching library while EasyMatch is a gray-level and color pattern-matching library. This paper proposes a high-speed gray pattern match algorithm especially for the automatic alignment system in lithography tools. The process of automatic alignment with machine vision and image processing algorithms are described in detail. The CCD calibration relating the image coordinate to the world coordinate is also analyzed, and a dynamic calibration algorithm applicable to the automatic alignment system is presented.

2. METHODOLOGY

2.1 Automatic alignment process

Figure 1 depicts the process of automatic alignment for lithography tools including five main machine vision algorithms, namely image enhancement algorithm, template learning algorithm, template matching algorithm, calibration algorithm, and coordinate transformation algorithm. The first step, known as image pre-processing and enhancement algorithm is mainly directed against the image noise by smoothing. The second step processes the image to find the feature location in pixels using high-speed gray pattern match algorithms. In the final step, the location in the world coordinate system is estimated by results of CCD camera calibration and used to reject the results if the quality of machine vision system is

* Contact author: shyliu@mail.hust.edu.cn; phone: +86 27 87792409; fax: +86 27 87792413.

4th International Symposium on Advanced Optical Manufacturing and Testing Technologies: Design, Manufacturing, and Testing of Micro- and Nano-Optical Devices and Systems, edited by Sen Han, Masaomi Kameyama, Xiangang Luo
Proc. of SPIE Vol. 7284, 72840I · © 2009 SPIE · CCC code: 0277-786X/09/$18 · doi: 10.1117/12.832076

inadequate to deliver the required accuracy.

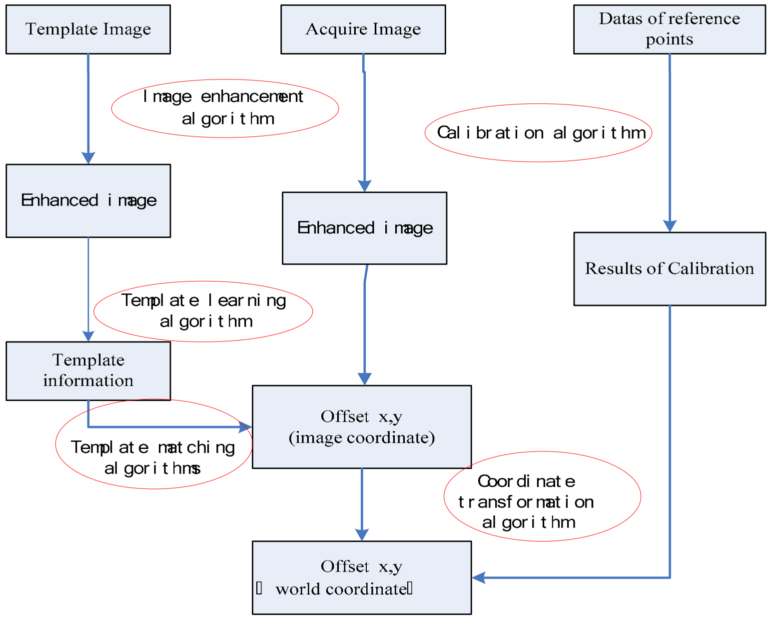

Fig.1. Automatic alignment process with machine vision algorithms for lithography tool

2.2 High-speed gray pattern match algorithm

A high-speed gray pattern match algorithm is proposed based on the combination of sequential similarity detection algorithm (SSDA) and multiresolution pagoda structure algorithm (MPSA). The overall matching process of the algorithm uses the pyramid approach in MPSA, while the search operation is performed from low-resolution images to high-resolution images by a cumulative value operator similarly used in SSDA. Absolute error of each pixel location (i, j) is defined as in Equation (1), accumulated errors of each match point is defined as in Equation (2), and in each position the cross correlation coefficient *R(i, j)* between the template image and the corresponding part of the search image is computed according to Equation (3).

$$\varepsilon(i,j,m,n) = \left| S(i+m, j+n) - S_{av}^{ij} - T(m,n) + T_{av} \right| \tag{1}$$

$$E(i,j) = \sum_{n=0}^{n} \sum_{m=0}^{m} \varepsilon(m,n) \tag{2}$$

$$R(i,j) = \frac{\sum_{(m,n)\in W} [S(i+m, j+n) - S_{av}^{i,j}][T(m,n) - T_{av}]}{\sqrt{\sum_{(m,n)\in W} [S(i+m, j+n) - S_{av}^{i,j}]^2 \sum_{(m,n)\in W} [T(m,n) - T_{av}]^2}} \tag{3}$$

where $S(i{+}m,\ j{+}n)$ is individual gray value of corresponding part of the search matrix, S_{av}^{ij} is average gray value of corresponding part of the search matrix, $T(m,\ n)$ is individual gray value of the template matrix, T_{av} is average gray value of the template matrix, m and n are number of rows and columns of the template matrix, respectively. The position of the best matching is determined by Algorithm 1.

Algorithm 1. High-speed gray pattern match algorithm

Step 1. Set resolution of image matching and the search area.
Step 2. Set threshold of match accumulated errors Et.
Step 3. Calculate accumulated error for the next match point.
Step 4. Calculate absolute error of each pixel.
Step 5. Calculate current accumulated match point error E. If E<Et, go to Step 6; if E>Et, jump out of this point, go to Step 3.
Step 6. If not completing calculation of all the pixels in the templates image, go to Step 4. If so, use current accumulated errors E to replace Et and record the location of the match point.
Step 7. If not traversing the whole image search, go to Step 3.
Step 8. If the image resolution does not meet the original image resolution, go to Step 1, else the best matching position (i, j) is obtained by the minimum of the accumulated error.
Step 9. Calculate the cross correlation coefficient of the best match position. If the value>0.7, calculate the best match point in sub-pixel resolution, else return an unsuccessful matching message.

The proposed algorithm is based on the image pyramid approach in which the resolution from one level to the next is reduced by a factor of 2. The matching process is performed from coarse to fine, and the results achieved on one resolution are considered as approximations for the next finer level. A coarser resolution is equivalent to a smaller image scale and a larger pixel size. Then the cross correlation coefficient of the best match position and its eight neighboring points are computed by Equation (3). The best match point in sub-pixel resolution can be extracted by the least square surface fitting method defined in Equation (4).

$$R(x,y) = ax^2 + bxy + cy^2 + dx + ey + f \tag{4}$$

where the parameters a, b, c, d, e and f are factors to be determined. According to the least square fitting theory of nonlinear functions, values of factors a, b, c, d, e and f can be calculated using scattered data of the best match position and its eight neighboring points. The location of the surface extreme point can be deduced from the values of above factors using Equation (5).

$$\begin{cases} x_0 = \dfrac{2cd - be}{b^2 - 4ac} \\ y_0 = \dfrac{2ae - bd}{b^2 - 4ac} \end{cases} \tag{5}$$

2.3 Dynamic camera calibration algorithm

Camera calibration in the context of machine vision is the process of determining the internal camera geometric and optical characteristics (intrinsic parameters) and position of the camera frame relative to a certain world coordinate system (extrinsic parameters). Here a high-precision X-Y stage is proposed for dynamic calibration. To accurately estimate the radial lens distortion, the calibration data should be distributed broadly across the field of view. Figure 2 shows the movement of stage in X-Y directions. The location in sub-pixel resolution of the template image is calculated in the field of view, the location in stage coordinates is recorded, and a series of points suitable for system calibration is obtained.

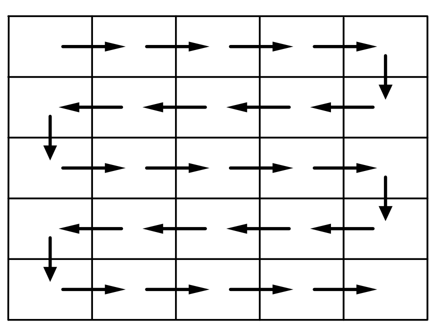

Fig.2. Movement of high-precision stage in X-Y directions for dynamic calibration

The Tsai's calibration procedure consists of two steps. In the first step, the external parameters are estimated. In the second step, the camera's internal geometry and optical properties are estimated. There are six extrinsic parameters including three components for the translation vector t, and the Euler angles yaw θ, pitch φ, and tilt ψ for rotation. The five intrinsic parameters include:

f_r Effective focal length, or image plane to projective center distance;
k_1 1st order radial lens distortion coefficient;
S_x Scale factor to account for any uncertainty in the frame grabber's resampling of the horizontal scan line;
(Cx, Cy) computer image coordinate for the origin in the image plane.

Since all calibration points are on a common plane, Tsai's algorithm for coplanar data is used. The single plane case does not calibrate parameters S_x and (Cx, Cy) can be simply considered to be the center pixel of the frame buffer. In addition to the 11 variable camera parameters Tsai's model has six fixed intrinsic camera constants:

N_{cx} Number of sensor elements in camera's X direction (in sels);
N_{fx} Number of pixels in frame grabber's X direction (in pixels),
dx Center to center distance between adjacent sensor elements in X (scan line) direction (in mm/sel);
dy Center to center distance between adjacent sensor elements in Y direction (in mm/sel);
dpx Effective X dimension of pixel in frame grabber (in mm/pixel);
dpy Effective Y dimension of pixel in frame grabber (in mm/pixel).

The rough steps of the dynamic camera calibration process based on Tsai's are shown in Algorithm 2.

Algorithm 2. Dynamic camera calibration algorithm

Step 1. Transform each calibration data from image coordinate (X_{fi}, Y_{fi}) to camera coordinate (X_{di} , Y_{di}) in mm by Equation (6).
Step 2. Calculate the five unknowns $r_1/t_y, r_2/t_y, t_x/t_y, r_4/t_y, r_5/t_y$ by Equation (7), where (x_{wj}, y_{wj}, z_{wj}) is the 3D object coordinate.
Step 3. Calculate (R, t_x, t_y) from five unknowns $r_1/t_y, r_2/t_y, t_x/t_y, r_4/t_y, r_5/t_y$ by Equation (8), where R is a 3×3 rotation matrix, and t_x and t_y are two elements of the translation vector t.
Step 4. Calculate an approximation of f_r and t_z by ignoring lens distortion.
Step 5. Obtain an exact solution for f_r, t_z, k_1.

The mainly involved equations used in the calibration are listed below, and the detailed information can be referred to reference [10].

$$\begin{cases} X_{di} = dpx \cdot (X_{fi} - Cx) = dx \dfrac{N_{cx}}{N_{fx}} (X_{fi} - Cx) \\ Y_{di} = dpy \cdot (Y_{fi} - Cy) = dy (Y_{fi} - Cy) \end{cases} \tag{6}$$

$$\begin{bmatrix} X_{di} x_{wi} & X_{di} y_{wi} & Y_{di} & -X_{di} x_{wi} & -X_{di} y_{wi} \end{bmatrix} \begin{bmatrix} t_y^{-1} r_1 \\ t_y^{-1} r_2 \\ t_y^{-1} t_x \\ t_y^{-1} r_4 \\ t_y^{-1} r_5 \end{bmatrix} = X_{di} \tag{7}$$

$$R = \begin{pmatrix} r_1 & r_2 & r_3 \\ r_4 & r_5 & r_6 \\ r_7 & r_8 & r_9 \end{pmatrix} = \begin{pmatrix} \cos\psi\cos\theta & \sin\psi\cos\theta & -\sin\theta \\ -\sin\psi\cos\phi + \cos\psi\sin\theta\cos\phi & \cos\psi\cos\phi + \sin\psi\sin\theta\sin & \cos\theta\sin\phi \\ \sin\psi\sin\phi + \cos\psi\sin\theta\cos\phi & -\cos\psi\sin\phi + \sin\psi\sin\theta\cos\phi & \cos\theta\cos\phi \end{pmatrix} \tag{8}$$

3. EXPERIMENTS

Based on above methodology, a machine vision algorithm library called AL_IP has been developed. An experimental platform for automatic alignment system has also been set up, including a light source, an optical system, a CCD camera, an image grabber card, a high-precision X-Y stage and other components. A halogen light is used as the light source, and a Navitar Zoom 6000 is adopted as the optical system. The matrix CCD is Pulnix CCD camera TM-1020-CL with an imaging resolution of 1008×1018. A high-performance image grabber, Euresys GrabLink Expert 2 cPCI, is used to obtain the CCD image. The positioning accuracy of the X-Y stage for dynamic calibration test is 50nm. The entire automatic alignment system is isolated from the ground vibration by an active damping system STACIS2000 from TMC.

A lot of experiments have been carried out to verify the performance of the proposed real-time gray-based template match algorithm. A selected template image with 108×114 pixels is shown in Fig.3 and one of the search images with 108×1018 pixels is shown in Fig.4. Table 1 depicts the comparison using library AL_IP and eVision. The later is a commercial image processing software developed by Euresys Company. It includes a template matching module called EasyMatch, which is claimed to be able to achieve a matching accuracy of one-twentieth of pixels. Figures 5 and 6 show the compared match error in X and Y directions, respectively. It is clearly observed that all of the position match errors are within 0.1 pixels.

Table 1. Match results using library AL_IP and eVsion

No.	Match results with AL_IP in X direction (pixels)	Match results with eVision in X direction (pixels)	Error in X direction (pixels)	Match results with AL_IP in Y direction (pixels)	Match results with eVision in Y direction (pixels)	Error in Y direction (pixels)	Error in total (pixels)
1	483.28	483.28	0.00	481.59	481.59	0.00	0.00
2	488.28	488.27	0.01	485.06	485.05	0.01	0.01
3	493.39	493.41	-0.02	488.65	488.71	-0.06	0.06
4	498.41	498.37	0.04	492.32	492.38	-0.06	0.07
5	503.29	503.28	0.01	495.78	495.78	0.00	0.01
6	508.31	508.29	0.02	499.24	499.22	0.02	0.03
7	513.47	513.47	0.00	502.76	502.78	-0.02	0.02
8	518.33	518.34	-0.01	506.49	506.48	0.01	0.01
9	523.40	523.39	0.01	509.91	509.91	0.00	0.01
10	528.33	528.38	-0.05	513.40	513.37	0.03	0.06

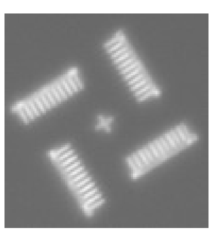

Fig.3. Selected template image with 108×114 pixels

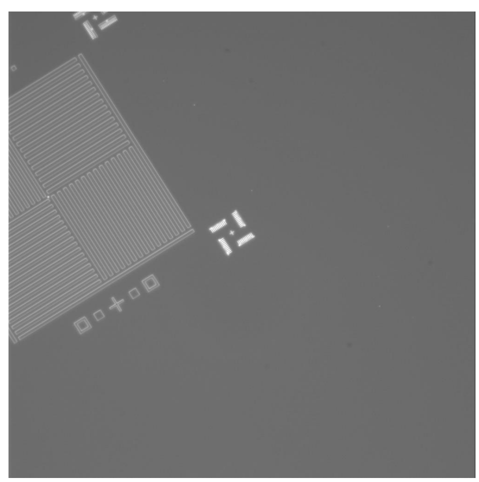

Fig.4. Searching image with 1008×1018 pixels

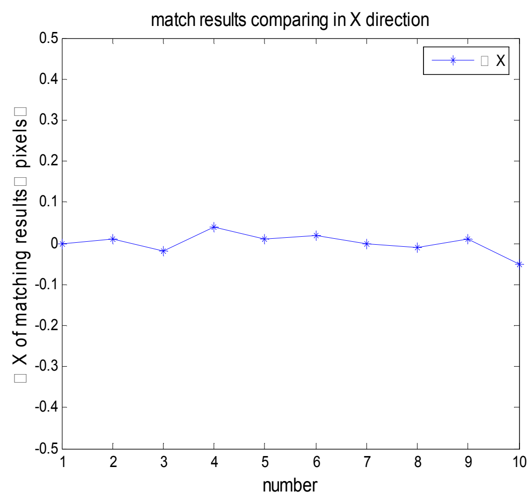

Fig.5. Match error in X direction

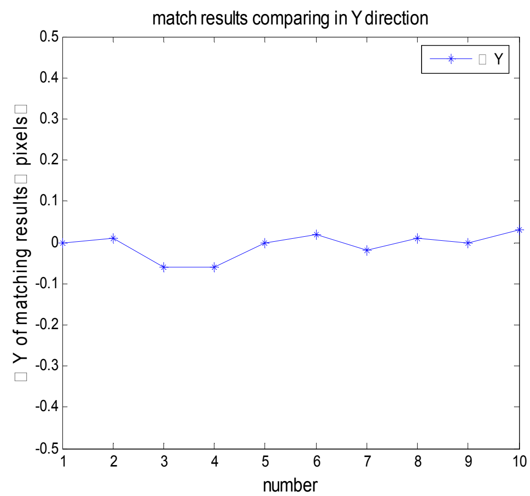

Fig.6. Match error in Y direction

Table 2 shows the average matching time with library AL_IP on different computer platforms. When using a large template image with 320×320 pixels, the matching time is demonstrated to be shorter than 80ms on a Dell 630m PC with a 1.73GHz CPU, a 512M memory and Windows operation system, while it is shown to be shorter than 200ms on a Power PC with a 500MHz CPU, a 512M memory, and VxWorks operation system.

Table 2. Matching time with AL_IP on different computer

Size of template image	Average matching time on Power PC (ms)	Average matching time on Dell 630m (ms)
60×60	50	33
100×100	50	33
200×200	116	33
320×320	197	67

Table 3 shows the results of system calibration with library AL_IP, and Table 4 depicts the alignment errors after calibration. It illustrates that the absolute alignment error is lower than 200nm both in X and Y directions within a large field of view of 1mm×1mm after the platform is calibrated using the proposed dynamic calibration method.

Table 3. Results of system calibration using the proposed dynamic calibration method

Rotation matrix	r_1	0.165891	Translation vector	t_x	475.842302 (μm)
	r_2	0.986139		t_y	303.482808 (μm)
	r_3	0.003059		t_z	-21507.691455 (μm)
	r_4	0.967699	Rotation angles	θ	80.450976°
	r_5	-0.163384		φ	11.069559°
	r_6	0.192000		ψ	-0.175242°
	r_7	0.189838	Effective focal length	f_r	170871.665139 (μm)
	r_8	-0.028891	Distortion coefficient	k_1	1.08×10^{-10}
	r_9	-0.981390	Magnification factor	M	7.944677

Table 4. Calculated alignment error after calibration

No.	Measured stage position		Calculated alignment position				Calculated step error	
	X direction (μm)	Y direction (μm)	X direction (pixels)	X direction (μm)	Y direction (pixels)	Y direction (μm)	X direction (μm)	Y direction (μm)
1	-350.05	-400.00	483.28	-349.573	481.59	-400.068		

2	-355.00	-405.05	488.28	-354.491	485.06	-405.086	-4.918	-5.018
3	-360.00	-410.00	493.39	-359.573	488.65	-410.212	-5.082	-5.126
4	-365.00	-415.00	498.41	-364.726	492.32	-415.220	-5.153	-5.008
5	-369.95	-420.00	503.29	-369.609	495.78	-420.109	-4.883	-4.889
6	-375.00	-425.00	508.31	-374.529	499.24	-425.160	-4.920	-5.051
7	-380.00	-430.00	513.47	-379.534	502.76	-430.351	-5.005	-5.191
8	-385.00	-434.95	518.33	-384.726	506.49	-435.166	-5.192	-4.815
9	-390.00	-440.05	523.40	-389.601	509.91	-440.275	-4.875	-5.109
10	-395.00	-445.00	528.33	-394.537	513.40	-445.218	-4.936	-4.943

4. CONCLUSIONS

Through a lots of experiments conducted on a testing platform, the automatic alignment system based on machine vision is proven to be feasible and effective. The experimental results show that the developed library AL_IP has high accuracy and fast computation speed. The pattern match function has equivalent precision compared with the commercial software eVision, and the computation time is shorter than 200ms when using a large template image with 320×320 pixels. The absolute alignment error is lower than 200nm after the platform is calibrated. It is expected that this technique will provide a useful practical tool for the automatic alignment in product optical lithography tools as well as other applications.

ACKNOWLEDGMENTS

This project is funded by Hi-Tech Research and Development Program of China (Grant No. 2006AA04Z325), National Natural Science Foundation of China (Grant No. 50775090) and Program for New Century Excellent Talents in University of China (Grant No. NCET-06-0639).

REFERENCES

1. Gliech, S., Steinert, J., and Duparre, A., "Light-scattering measurement of optical thin-film components at 157 and 193nm", Applied Optics 41, 3224-3234 (2002).
2. Nitzsche, G., Rild, R., Altenburger, U., et al, "Optical image processing - a useful tool in wafer inspection", Microelectronic Engineering 23, 391-394 (1994).
3. Giles, D. K. and Slaughter, D. C., "Precision band spraying with machine-vision guidance and adjustable yaw nozzles", Trans. ASAE 40, 29-36 (1997).
4. Wagner, C., Kaiser, W., MulKens, J., et al, "Advance technology for extending optical lithography", Proc. SPIE 4000, 344-357 (2000).
5. Schoot, J., Bornebroek, F., Suddendorf, M., et al, "0.7 NA DUV step & scan system for 150nm imaging with improved overlay", Proc. SPIE 3679, 448-463 (1999).
6. Gabeli, F., Huber, H., Kucinski, A., et al, "Alignment and overlay accuracy of an advanced X-ray stepper using an improved alignment system", Proc. SPIE 1671, 401-411, 1992.
7. Barnea, D. I. and Silverman, H. F., "A class of algorithms for fast digital image registration", IEEE Trans. Computers 21, 179-186 (1972).
8. Parker, A. J., Kenyon, R.V., and Troxel, D., "Comparison of interpolating methods for image resampling", IEEE Trans. Medical Imaging 2, 31-39 (1983).
9. Schurz, D., Flack, W., and Hsieh, R., "Dual side lithography measurement precision and accuracy", Proc. SPIE 5752, 904-911 (2005).
10. Tsai, R., "A versatile camera calibration technique for high-accuracy 3d machine vision metrology using off-the-shelf TV cameras and lenses", IEEE J. Robotics Automation 3, 323-344 (1987).